Direct Lanthanide−Transition Metal Interactions: Synthesis of $(NH_3)_2YbFe(CO)_4$ and Crystal Structures of $\{[(CH_3CN)_3YbFe(CO)_4]_2\cdot CH_3CN\}_\infty$ and $[(CH_3CN)_3YbFe(CO)_4]_\infty$

Haibin Deng,† Sung-Ho Chun, Pierre Florian, Philip J. Grandinetti, and Sheldon G. Shore*

Department of Chemistry, The Ohio State University, Columbus, Ohio 43210

Received November 22, 1995⊗

The heterometallic complex $(NH_3)_2YbFe(CO)_4$ was prepared from the reduction of $Fe_3(CO)_{12}$ by Yb in liquid ammonia. Ammonia was displaced from $(NH_3)_2YbFe(CO)_4$ by acetonitrile in acetonitrile solution, and the crystalline compounds $\{[(CH_3CN)_3YbFe(CO)_4)]_2\cdot CH_3CN\}_\infty$ and $[(CH_3CN)_3YbFe(CO)_4]_\infty$ were obtained. An earlier X-ray study of $\{[(CH_3CN)_3YbFe(CO)_4]_2\cdot CH_3CN\}_\infty$ showed that it is a ladder polymer with direct Yb−Fe bonds. In the present study, an X-ray crystal structure analysis also showed that $[(CH_3CN)_3YbFe(CO)_4]_\infty$ is a sheetlike array with direct Yb−Fe bonds. Crystal data for $\{[(CH_3CN)_3YbFe(CO)_4]_2\cdot CH_3CN\}_\infty$: monoclinic space group $P2_1/c$, $a = 21.515(8)$ Å, $b = 7.838(2)$ Å, $c = 19.866(6)$ Å, $\beta = 105.47(2)°$, $Z = 4$. Crystal data for $[(CH_3CN)_3YbFe(CO)_4]_\infty$: monoclinic space group $P2_1/n$, $a = 8.364(3)$ Å, $b = 9.605(5)$ Å, $c = 17.240(6)$ Å, $\beta = 92.22(3)°$, $Z = 4$. Electrical conductivity measurements in acetonitrile show that these acetonitrile complexes are partially dissociated into ionic species. IR and NMR spectra of the solutions reveal the presence of $[HFe(CO)_4]^-$. However, upon recrystallization, the acetonitrile complexes show no evidence for the presence of $[HFe(CO)_4]^-$ on the basis of their IR spectra. The solid state MAS ^2H NMR spectra of deuterated acetonitrile complexes give no evidence for $[^2HFe(CO)_4]^-$. It appears that rupture of the Yb−Fe bond could occur in solution to generate the ion pair $[L_nYb]^{2+}[Fe(CO)_4]^{2-}$, but then the highly basic $[Fe(CO)_4]^{2-}$ anion could abstract a proton from a coordinated acetonitrile ligand to form $[HFe(CO)_4]^-$. However, upon crystallization, the proton could be transferred back to the ligand, which results in the neutral polymeric species.

Introduction

Metal−metal bonds are one of the principal themes of molecular organometallic and cluster chemistry.[1] Bonds between transition metals are most common. However, metal−metal bonds between transition metals and electropositive elements, such as alkali,[2] alkaline earth,[3] lanthanide,[4,5] and actinide elements[6] are relatively rare. Direct transition metal−lanthanide bonds have been largely inferred from infrared and NMR spectroscopic data,[4] while X-ray diffraction studies are scarce. A Lu^{3+} to Ru bond (2.955 Å) in $[Cp_2(THF)LuRu(CO)_2Cp]$ has been reported.[5a,b] In a preliminary report,[7] we described the first example of metal−metal bonding involving a divalent lanthanide and a transition metal element. In this paper, we provide additional examples of such complexes and give a full account of their synthesis and structural characterization.

Our strategy for the synthesis of compounds containing direct transition metal−lanthanide bonds is to utilize divalent lanthanides and highly reduced transition metal centers, the former being softer Lewis acids than their trivalent counterparts[8] and the latter being soft Lewis bases and excellent nucleophiles.[9] In cases where transition metal centers are not sufficiently nucleophilic, the lanthanide ions either are surrounded by coordinating solvents, forming solvent-separated ion pairs with transition metal carbonylates,[10] or are coordinated by carbonyl oxygens of the transition metal carbonylates, forming isocarbonyl linkages.[11]

We describe here the reduction of the neutral transition metal carbonyl $Fe_3(CO)_{12}$ by the lanthanide element ytterbium in liquid ammonia. Details of the synthesis and characterization of $(NH_3)_2YbFe(CO)_4$, $\{[(CH_3CN)_3YbFe(CO)_4]_2\cdot CH_3CN\}_\infty$, and

† Deceased.

⊗ Abstract published in *Advance ACS Abstracts,* June 1, 1996.

(1) (a) *The Chemistry of Metal Cluster Complexes*; Shriver, D. F., Kaesz, H. D., Adams, R. D., Eds.; VCH Publishers, Inc.: New York, 1990. (b) *Introduction to Cluster Chemistry*; Mingos, D. M. P., Wales, D. J., Eds.; Prentice-Hall, Inc.: London, 1990.

(2) See, for example: Fryzuk, M. D.; Lloyd, B. R.; Clentsmith, G. K. B.; Rettig, S. J. *J. Am. Chem. Soc.* **1991**, *113*, 4332.

(3) See, for example: (a) Felkin, H.; Knowles, P. J.; Meunier, B. *J. Chem. Soc., Chem. Commun.* **1974**, 44. (b) McVicker, G. B. *Inorg. Chem.* **1975**, *14*, 2087.

(4) (a) Marianelli, R. S.; Durney, M. T. *J. Organomet. Chem.* **1971**, *32*, C41. (b) Marks, T. J.; Kristoff, J. S.; Alich, A.; Shriver, D. F. *J. Organomet. Chem.* **1971**, *33*, C35. (c) Crease, A. E.; Legzdins, P. *J. Chem. Soc., Dalton Trans.* **1973**, 1501. (d) Onaka, S.; Furuichi, N. *J. Organomet. Chem.* **1979**, *173*, 77. (e) Beletskaya, I. P.; Suleimanov, G. Z.; Shifrina, R. R.; Mekhdiev, R. Y.; Agdamskii, T. A.; Khandozhko, V. N.; Kolobova, N. E. *J. Organomet. Chem.* **1986**, *299*, 239. (f) Beletskaya, I. P.; Voskoboinikov, A. A.; Magomedov, G. K. I. *Metalloorg. Khim.* **1990**, *3*, 516 and references therein.

(5) (a) Magomedov, G. K.; Voskoboynikov, A. Z.; Chuklanova, E. B.; Gusev, A. I.; Beletskaya, I. P. *Metalloorg. Khim.* **1990**, *3*, 706. (b) Beletskaya, I. P.; Voskoboynikov, A. Z.; Chuklanova, E. B.; Kirillova, N. I.; Shestakova, A. K.; Parshina, I. N.; Gusev, A. I.; Magomedov, G. K.-I. *J. Am. Chem. Soc.* **1993**, *115*, 3156. (c) Suleimanov, G. Z.; Mechdiev, R. Y.; Kurbanov, T. K.; Trunov, V. G.; Beletskaya, I. P. *Abstracts of Papers,* International Rare Earth Conference, Zurich, 1985; J6. (d) Alvarez, D., Jr.; Caulton, K. G.; Evans, W. J.; Ziller, J. W. *J. Am. Chem. Soc.* **1990**, *112*, 5674.

(6) (a) Bennett, R. L.; Bruce, M. I.; Stone, F. G. A. *J. Organomet. Chem.* **1971**, *26*, 355. (b) Ritchey, J. M.; Zozulin, A. J.; Wrobleski, D. A.; Ryan, R. R.; Wasserman, H. J.; Moody, D. C.; Paine, R. T. *J. Am. Chem. Soc.* **1985**, *107*, 501. (c) Sternal, R. S.; Brock, C. P.; Marks, T. J. *J. Am. Chem. Soc.* **1985**, *107*, 8270. (d) Hay, P. J.; Ryan, R. R.; Salazar, K. V.; Wrobleski, D. A.; Sattelberger, A. P. *J. Am. Chem. Soc.* **1986**, *108*, 313. (e) Ortiz, J. V. *J. Am. Chem. Soc.* **1986**, *108*, 550. (f) Bursten, B. E.; Novo-Gradac, K. J. *J. Am. Chem. Soc.* **1987**, *109*, 904. (g) Sternal, R. S.; Sabat, M.; Marks, T. J. *J. Am. Chem. Soc.* **1987**, *109*, 7920. (h) Sternal, R. S.; Marks, T. J. *Organometallics* **1987**, *6*, 2621.

(7) Deng, H.; Shore, S. G. *J. Am. Chem. Soc.* **1991**, *113*, 8538.

(8) Pearson, R. G. *J. Am. Chem. Soc.* **1963**, *85*, 3533.

(9) Ellis, J. E. *Adv. Organomet. Chem.* **1990**, *31*, 1.

(10) (a) Evans, W. J.; Bloom, I.; Grate, J. W.; Hughes, L. A.; Hunter, W. E.; Atwood, J. L. *Inorg. Chem.* **1985**, *24*, 4620. (b) Beletskaya, I. P.; Voskoboynikov, A. Z.; Chuklanova, E. B.; Gusev, A. I.; Magomedov, G. K. *Metalloorg. Khim.* **1988**, *1*, 1383. (c) White, J. P., III. Ph.D. Dissertation, The Ohio State University, Columbus, OH, 1990. (d) Deng, H. Ph.D. Dissertation, The Ohio State University, Columbus, OH, 1991.

S0020-1669(95)01511-4 CCC: $12.00

$[(CH_3CN)_3YbFe(CO)_4]_\infty$ are described. Crystal structures of the acetonitrile complexes confirm the presence of direct metal−metal bonds between a divalent Yb^{2+} ion and a formal Fe(−II) atom.

Results and Discussion

Preparation of $(NH_3)_2YbFe(CO)_4$, $\{[(CH_3CN)_3YbFe(CO)_4]_2\cdot CH_3CN\}_\infty$, and $[(CH_3CN)_3YbFe(CO)_4]_\infty$. Ytterbium is a strong reducing agent in liquid ammonia. It ionizes to give Yb^{2+} and solvated electrons.[12] The ammonia solution reduces $Fe_3(CO)_{12}$ to form an iron carbonylate salt of ytterbium according to eq 1.[7]

$$3Yb + Fe_3(CO)_{12} \xrightarrow{NH_3(l)} 3(NH_3)_2YbFe(CO)_4 \qquad (1)$$

The solid compound isolated from this reaction after prolonged residence under dynamic vacuum contains approximately two NH_3 molecules per Yb atom, as determined by elemental analysis. It is an extremely air- and moisture-sensitive yellow solid which sometimes catches fire instantly upon exposure to air. It is not soluble in hydrocarbon or ether solvents. It is slightly soluble in acetonitrile, but the NH_3 ligands are displaced by CH_3CN molecules. Noticeable decomposition of the acetonitrile solutions is observed after several hours at room temperature.

While solutions of $(NH_3)_2YbFe(CO)_4$ in acetonitrile are unstable at room temperature, displacement of ammonia ligands by acetonitrile at low temperature produces discrete, isolable single crystals of $\{[(CH_3CN)_3YbFe(CO)_4]_2\cdot CH_3CN\}_\infty$ and $[(CH_3CN)_3YbFe(CO)_4]_\infty$. These acetonitrile complexes are orange and are also highly air sensitive.

Structures of $\{[(CH_3CN)_3YbFe(CO)_4]_2\cdot CH_3CN\}_\infty$ and $[(CH_3CN)_3YbFe(CO)_4]_\infty$. From single-crystal X-ray analyses, the molecular structures of $\{[(CH_3CN)_3YbFe(CO)_4]_2\cdot CH_3CN\}_\infty$ and $[(CH_3CN)_3YbFe(CO)_4]_\infty$ were determined. The structure of $\{[(CH_3CN)_3YbFe(CO)_4]_2\cdot CH_3CN\}_\infty$ was briefly described in a preliminary communication.[7] It consists of "polymeric ladders" extending along the crystallographic *b* axis of the lattice. Figure 1 shows an ORTEP drawing of a portion of a ladder. Figure 2a displays the coordination geometries of the Fe and Yb atoms. The $Fe(CO)_4$ units have distorted trigonal-bipyramidal geometries, while those of the Yb^{2+} ions are distorted octahedra. In addition to three CH_3CN ligands, each Yb^{2+} ion is coordinated to two carbonyl oxygens from two different $Fe(CO)_4$ units; each $Fe(CO)_4$ unit is in turn connected to two different Yb^{2+} ions *via* isocarbonyl linkages, thus forming a zigzag ···Yb−O−C−Fe−C−O−Yb··· chain. Two such chains are coupled to form a ladder through Yb−Fe interactions. The Yb−Fe distance is 3.010(1) Å.

The X-ray structure of $[(CH_3CN)_3YbFe(CO)_4]_\infty$ consists of "polymeric sheets" stacked perpendicular to the crystallographic *c* axis. Figure 3 shows ORTEP drawings of a portion of the sheet. Figure 2b displays the coordination geometries of the Fe and Yb atoms. Crystal data and selected bond distances and angles for both structures are reported in Tables 1 and 2,

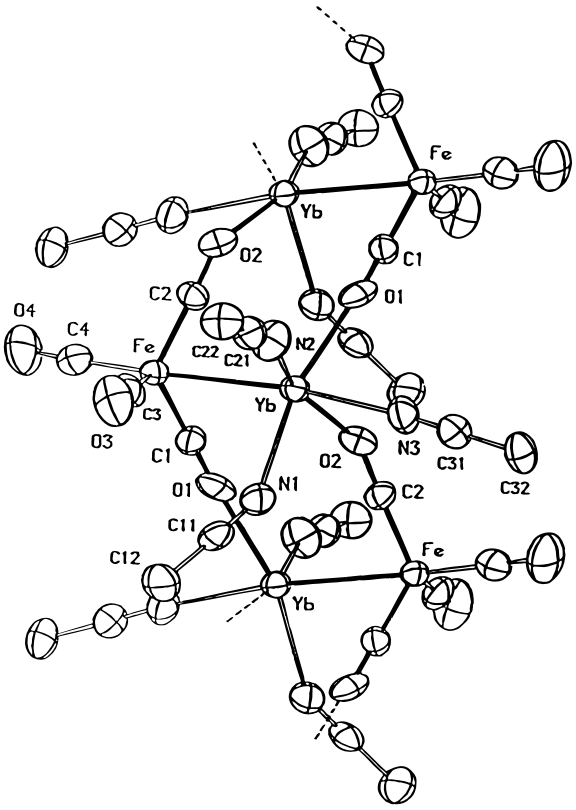

Figure 1. Molecular structure of $\{[(CH_3CN)_3YbFe(CO)_4]_2\cdot CH_3CN\}_\infty$.

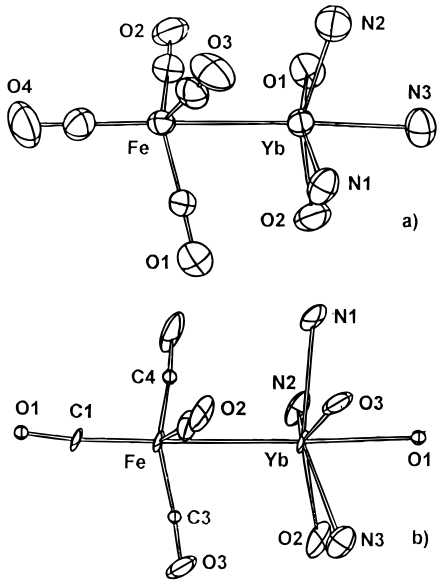

Figure 2. Coordination geometries of Yb and Fe in (a) $\{[(CH_3CN)_3YbFe(CO)_4]_2\cdot CH_3CN\}_\infty$ and (b) $[(CH_3CN)_3YbFe(CO)_4]_\infty$.

respectively. The structure of $[(CH_3CN)_3YbFe(CO)_4]_\infty$ is closely related to that of $\{[(CH_3CN)_3YbFe(CO)_4]_2\cdot CH_3CN\}_\infty$ in that the polymeric ladders are cross-linked by extra Fe−C−O−Yb isocarbonyl linkages to form the sheet (Scheme 1). The coordination geometry of Yb^{2+} is that of a distorted pentagonal bipyramid that results from additional isocarbonyl coordination from the neighboring "ladder". The geometries of the $Fe(CO)_4$ units in $[(CH_3CN)_3YbFe(CO)_4]_\infty$ are similar to those in $\{[(CH_3CN)_3YbFe(CO)_4]_2\cdot CH_3CN\}_\infty$. The Yb−Fe bond distance, 3.046(1) Å, is slightly longer than the corresponding distance in $\{[(CH_3CN)_3YbFe(CO)_4]_2\cdot CH_3CN\}_\infty$. Yb−Fe, Yb−O, and Yb−N bond distances in $[(CH_3CN)_3YbFe(CO)_4]_\infty$ are also slightly longer than those in $\{[(CH_3CN)_3YbFe(CO)_4]_2\cdot CH_3CN\}_\infty$ due

(11) (a) Tilley, T. D.; Andersen, R. A. *J. Chem. Soc., Chem. Commun.* **1981**, 985. (b) Tilley, T. D.; Andersen, R. A. *J. Am. Chem. Soc.* **1982**, *104*, 1772. (c) Boncella, J. M.; Andersen, R. A. *Inorg. Chem.* **1984**, *23*, 432. (d) Boncella, J. M.; Andersen, R. A. *J. Chem. Soc., Chem. Commun.* **1984**, 809. (e) Recknagel, A.; Steiner, A.; Brooker, S.; Stalke, D.; Edelmann, F. *Chem. Ber.* **1991**, *124*, 1373.

(12) (a) Warf, J. C.; Korst, W. L. *J. Phys. Chem.* **1956**, *60*, 1590. (b) Peer, W. J.; Lagowski, J. J. *J. Phys. Chem.* **1980**, *84*, 1110. (c) Thompson, J. C. *Electrons in Liquid Ammonia*; Oxford University Press: Oxford, U.K., 1976; p 230.

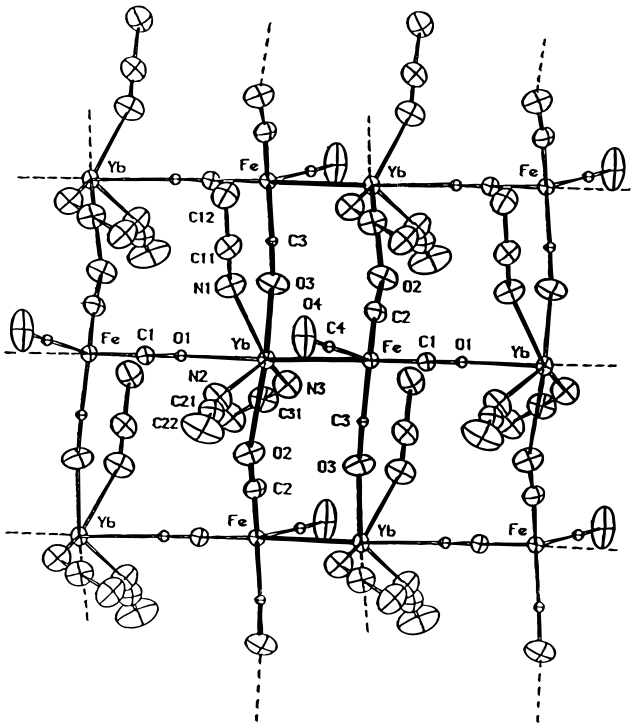

Figure 3. Molecular structure of $[(CH_3CN)_3YbFe(CO)_4]_\infty$.

Table 1. Crystallographic Data for $\{[(CH_3CN)_3YbFe(CO)_4]_2{\cdot}CH_3CN\}_\infty$ and $[(CH_3CN)_3YbFe(CO)_4]_\infty$

empirical formula	$C_{22}H_{21}Fe_2N_7O_8Yb_2$	$C_{10}H_9FeN_3O_4Yb$
fw	969.23	464.09
space group	$P2_1/c$	$P2_1/n$
a, Å	21.515(8)	8.364(3)
b, Å	7.838(2)	9.605(5)
c, Å	19.866(6)	17.240(6)
β, deg	105.47(2)	92.22(3)
V, Å^3	3228.7	1384.0
Z	4	4
ρ_{calcd}, g cm^{-3}	1.994	2.227
T, °C	−60	−60
λ, Å	0.710 73 (Mo Kα)	0.710 73 (Mo Kα)
μ, cm^{-1}	66.553	77.671
transm coeff	0.364−0.999	0.172−0.997
R_F[a]	0.031	0.064
R_{wF}[b]	0.040	0.078

[a] $R_F = \sum(|F_o| - |F_c|)/\sum|F_o|$. [b] $R_{wF} = \{\sum w(|F_o| - |F_c|)^2/\sum w|F_o|^2\}^{1/2}$, $w = [\sigma(F_o)^2 + (kF_o)^2]^{-1}$, $k = 0.04$.

to the higher coordination number of Yb^{2+} in $[(CH_3CN)_3YbFe(CO)_4]_\infty$.

The most salient features of these two structures are the direct Yb−Fe interactions and the distorted trigonal bipyramidal geometry of the Fe coordination sphere. The Yb−Fe distances of 3.010(1) Å in $\{[(CH_3CN)_3YbFe(CO)_4]_2{\cdot}CH_3CN\}_\infty$ and 3.046(1) Å in $[(CH_3CN)_3YbFe(CO)_4]_\infty$ are comparable to a Yb−Fe distance of 3.00 Å in $YbFe_2$ alloy.[13] They are 0.19 and 0.15 Å shorter than the sum of Yb and Fe metallic radii (3.2 Å),[14] respectively. This indicates a significant bonding interaction between Yb and Fe in both structures. Similarly, in $[Cp_2(THF)LuRu(CO)_2Cp]$ the direct Lu−Ru bond distance of 2.955 Å[5a] is 0.10 Å shorter than the sum of the Lu and Ru metallic radii (3.06 Å);[14] and in $[(C_5Me_5)_2(I)ThRu(CO)_2Cp]$ the direct Th−Ru bond distance (3.028 Å)[6c] is 0.11 Å shorter than the sum of Th and Ru metallic radii (3.14 Å).[14]

Table 2. Selected Bond Distances (Å) and Angles (deg) and Their Esd's for $\{[CH_3CN)_3YbFe(CO)_4]_2{\cdot}CH_3CN\}_\infty$[a] and $[(CH_3CN)_3YbFe(CO)_4]_\infty$

Distances

$\{[(CH_3CN)_3YbFe(CO)_4]_2{\cdot}CH_3CN\}_\infty$		$[(CH_3CN)_3YbFe(CO)_4]_\infty$	
Yb−Fe	3.0124(9)	Yb−Fe	3.046(1)
Yb−O1	2.380(5)	Yb−O1	2.444(8)
Yb−O2	2.374(5)	Yb−O2	2.541(6)
Yb−N1	2.509(7)	Yb−O3	2.459(6)
Yb−N2	2.487(7)	Yb−N1	2.553(8)
Yb−N3	2.531(6)	Yb−N2	2.539(9)
Fe−C1	1.729(7)	Yb−N3	2.560(9)
Fe−C2	1.715(7)	Fe−C1	1.73(1)
Fe−C3	1.769(8)	Fe−C2	1.73(1)
Fe−C4	1.754(8)	Fe−C3	1.74(1)
O1−C1	1.198(8)	Fe−C4	1.75(1)
O2−C2	1.198(8)	O1−C1	1.17(1)
O3−C3	1.157(9)	O2−C2	1.20(1)
O4−C4	1.163(8)	O3−C3	1.19(1)
N1−C11	1.124(9)	O4−C4	1.17(1)
N2−C21	1.14(1)	N1−C11	1.11(1)
N3−C31	1.132(9)	N2−C21	1.16(1)
C11−C12	1.45(1)	N3−C31	1.16(1)
C21−C22	1.44(1)	C11−C12	1.48(1)
C31−C32	1.44(1)	C21−C22	1.47(2)
N4−C41	1.12(1)	C31−C32	1.44(2)
C41−C42	1.46(1)		

Angles

$\{[(CH_3CN)_3YbFe(CO)_4]_2{\cdot}CH_3CN\}_\infty$		$[(CH_3CN)_3YbFe(CO)_4]_\infty$	
Fe−Yb−O1	105.5(1)	Fe−Yb−O1	177.7(1)
Fe−Yb−O2	103.4(1)	Fe−Yb−O2	101.7(2)
Fe−Yb−N1	89.4(1)	Fe−Yb−O3	100.6(2)
Fe−Yb−N2	99.1(2)	Fe−Yb−N1	95.3(2)
Fe−Yb−N3	172.4(2)	Fe−Yb−N2	94.6(2)
O1−Yb−O2	81.3(2)	Fe−Yb−N3	103.8(2)
O1−Yb−N1	164.7(2)	O1−Yb−O2	80.6(2)
O1−Yb−N2	93.8(2)	O1−Yb−O3	77.8(3)
O1−Yb−N3	82.0(3)	O1−Yb−N1	82.6(2)
O2−Yb−N1	92.1(2)	O1−Yb−N2	85.7(3)
O2−Yb−N2	157.4(2)	O1−Yb−N3	77.4(3)
O2−Yb−N3	78.8(2)	O2−Yb−O3	140.0(2)
N1−Yb−N2	87.1(2)	O2−Yb−N1	139.8(2)
N1−Yb−N3	83.2(2)	O2−Yb−N2	67.7(3)
N2−Yb−N3	78.7(2)	O2−Yb−N3	70.7(2)
Yb−Fe−C1	73.6(2)	O3−Yb−N1	69.4(3)
Yb−Fe−C2	75.0(2)	O3−Yb−N2	142.2(3)
Yb−Fe−C3	80.7(2)	O3−Yb−N3	71.9(3)
Yb−Fe−C4	175.7(3)	N1−Yb−N2	74.9(3)
C1−Fe−C2	118.7(3)	N1−Yb−N3	139.3(3)
C1−Fe−C3	111.7(3)	N2−Yb−N3	137.1(3)
C1−Fe−C4	105.5(3)	Yb−Fe−C1	174.8(3)
C2−Fe−C3	113.2(3)	Yb−Fe−C2	76.6(3)
C2−Fe−C4	102.2(3)	Yb−Fe−C3	76.1(3)
C3−Fe−C4	103.4(3)	Yb−Fe−C4	77.5(4)
Yb−O1−C1	168.4(5)	C1−Fe−C2	107.7(4)
Yb−O2−C2	134.8(6)	C1−Fe−C3	103.6(4)
Yb−N1−C11	160.7(6)	C1−Fe−C4	98.0(6)
Yb−N2−C21	162.0(7)	C2−Fe−C3	120.3(6)
Yb−N3−C31	170.8(7)	C2−Fe−C4	113.1(4)
Fe−C1−O1	177.7(6)	C3−Fe−C4	111.2(4)
Fe−C2−O2	176.8(6)	Yb−O1−C1	167.3(7)
Fe−C3−O3	178.7(8)	Yb−O2−C2	146.9(7)
Fe−C4−O4	178.3(7)	Yb−O3−C3	161.1(8)
N1−C11−C12	178.9(8)	Yb−N1−C11	157.1(8)
N2−C21−C22	178.4(9)	Yb−N2−C21	157.7(9)
N3−C31−C32	178.9(8)	Yb−N3−C31	136.4(8)
N4−C41−C42	178(1)	Fe−C1−O1	172.8(8)
		Fe−C2−O2	173.9(8)
		Fe−C3−O3	175.0(9)
		Fe−C4−O4	175(1)
		N1−C11−C12	180(2)
		N2−C21−C22	179(1)
		N3−C31−C32	176(1)

[a] Two crystallographically independent but stereochemically similar molecules were found in the crystal structure of $\{[(CH_3CN)_3YbFe(CO)_4]_2{\cdot}CH_3CN\}_\infty$. Only one set of bond distances and angles are listed here. See the supplementary material of ref 7 for full listings of bond distances and angles.

(13) Cannon, J. F.; Robertson, D. L.; Hall, H. T. *Mater. Res. Bull.* **1972**, *7*, 5.
(14) Wells, A. F. *Structural Inorganic Chemistry*, 5th ed.; Oxford University Press: New York, 1984; p 1288.

Scheme 1

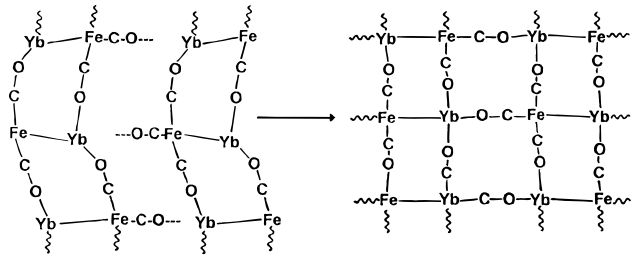

Chart 1

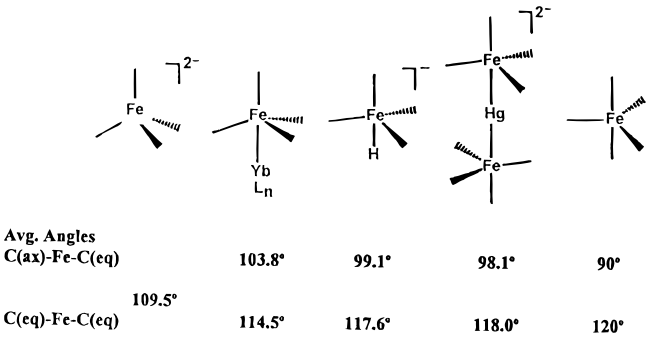

Chart 2

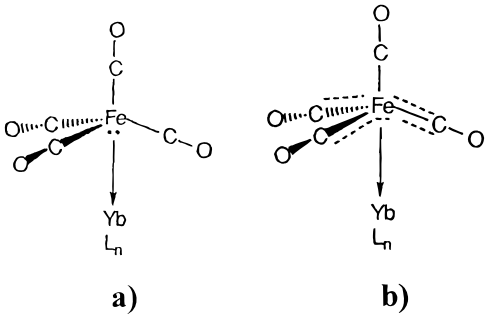

Distorted trigonal bipyramidal geometries are also found in $[HFe(CO)_4]^-$ [15] and $[Hg\{Fe(CO)_4\}_2]^{2-}$.[16] Changes in bond angles in proceeding from the Fe coordination sphere of a tetrahedron to a trigonal bipyramid are illustrated in Chart 1. The bond angles of $Fe(CO)_4$ in $\{[(CH_3CN)_3YbFe(CO)_4]_2\cdot CH_3CN\}_\infty$ and $[(CH_3CN)_3YbFe(CO)_4]_\infty$ are closer to tetrahedral symmetry, probably due to the predominantly ionic nature of the Yb−Fe bond.

Under C_{3v} symmetry, the d^{10} Fe atom in the $[Fe(CO)_4]^{2-}$ dianion should have an electron pair directed toward an axial site. The Yb−Fe bond can thus be described as a donor−acceptor interaction between the Fe center in $[Fe(CO)_4]^{2-}$ and Yb^{2+}, in spite of its high ionic character (Chart 2a). The concept of this type of dative bond between a low-valent transition metal center as the donor and an electropositive element as the acceptor in $[(C_5Me_5)_2(I)ThRu(CO)_2Cp]$ has been developed through the application of quasi-relativistic Xα−SW calculations.[6f]

Contacts between Yb^{2+} and carbonyl carbons of $[Fe(CO)_4]^{2-}$ are also observed in $\{[(CH_3CN)_3YbFe(CO)_4]_2\cdot CH_3CN\}_\infty$ and $[(CH_3CN)_3YbFe(CO)_4]_\infty$. The three Yb−C distances are 3.026(9), 3.073(8), and 3.201(9) Å in the former and 3.12(1), 3.13(1), and 3.17(1) Å in the latter. These distances are longer than the respective Yb−Fe bond distances, and the carbonyl groups involved are nearly linear, suggesting that there are only weak interactions between the Yb^{2+} ion and the three carbonyl carbons. Therefore, any contribution due to the trimethylenemethane-like coordination of the FeC_3 region of $[Fe(CO)_4]^{2-}$ to Yb^{2+} (Chart 2b) should be negligible compared to the direct Yb−Fe bonding, unlike that observed by Bau and co-workers in their study of $Na_2Fe(CO)_4\cdot 1.5(dioxane)$[17a] and $K_2Fe(CO)_4$.[17b] They showed that interactions between the alkali metal cation and the C−Fe−C regions may be described as that of a metal−allyl type.[17]

Other bond distances are in the normal range. Due to the high ionic character of the Yb^{2+}−ligand bonds, the bond distances increase as the coordination numbers increase. Thus the average Yb−N bond distance of 2.52[2][27] Å in $\{[(CH_3CN)_3YbFe(CO)_4]_2\cdot CH_3CN\}_\infty$ is comparable to that in $(CH_3CN)_4Yb(\mu\text{-}H)_3BH]_2$ (2.525[6] Å).[18] The average Yb−N bond distance of 2.55[1] Å in $[(CH_3CN)_3YbFe(CO)_4]_\infty$ is comparable with or shorter than those in $(CH_3CN)_6Yb(\mu\text{-}H)_2B_{10}H_{12}\cdot 2CH_3CN$ (2.55[3] Å),[19] $(C_5Me_5)_2Yb(C_5H_5N)_2$ (2.57[3] Å),[20] and $(C_8H_8)Yb(C_5H_5N)_3\cdot{}^1/_2C_5H_5N$ (2.58[2] Å).[21] The average Yb−O bond distances for the Yb−isocarbonyl linkages in $\{[(CH_3CN)_3YbFe(CO)_4]_2\cdot CH_3CN\}_\infty$ and $[(CH_3CN)_3YbFe(CO)_4]_\infty$ are 2.374[7] and 2.48[5] Å, respectively. The latter is comparable to those involving eight-coordinate trivalent Yb ions,[11a−d] due to the competing effects of coordination numbers and ionic radii on bond distances.

Interestingly, some of the Yb−N−C bond angles and Yb−O−C bond angles deviate substantially from linearity. The Yb−N−C bond angles range from 135 to 171°, and the Yb−O−C bond angles range from 135 to 168°. This phenomenon is also observed in a variety of compounds in which M−NCCH$_3$ coordination or M−isocarbonyl linkages are involved. It has been proposed that the angular position of the metal cation may allow interaction with electron density in both lone pairs and π orbitals on CH_3CN or isocarbonyls.[22] On the other hand, the energy gain or loss involved in the bending of the ligands might be sufficiently small that the crystal packing forces would suffice to cause the deviation of the M−N−C and M−O−C bonds from linearity. The Fe−C−O and N−C−C bond angles are close to 180°.

Proposed Structural Features of $(NH_3)_2YbFe(CO)_4$. Suitable crystals of $(NH_3)_2YbFe(CO)_4$ for X-ray analysis could not be produced. However, its essential structural features are likely to be similar to the main structural features of $\{[(CH_3CN)_3YbFe(CO)_4]_2\cdot CH_3CN\}_\infty$ and $[(CH_3CN)_3YbFe(CO)_4]_\infty$, on the basis of similarities in their IR spectra and their limited solubilities in acetonitrile. The Nujol mull IR spectrum of $(NH_3)_2YbFe(CO)_4$ in the carbonyl stretching region consists of three broad bands (1898 w, br, 1826 m, br, 1758 s, br cm^{-1}). This spectrum resembles the Nujol IR spectra of $\{[(CH_3CN)_3YbFe(CO)_4]_2\cdot CH_3CN\}_\infty$ (1890 w, br, 1781 m, br, 1720 s, br cm^{-1}) and $[(CH_3CN)_3YbFe(CO)_4]_\infty$ (1890, w, br, 1794 m, br, 1715 s, br cm^{-1}).

Thus the $Fe(CO)_4$ units in $(NH_3)_2YbFe(CO)_4$ are believed to be distorted tetrahedra of pseudo-C_{3v} symmetry (Chart 1), similar to the $Fe(CO)_4$ units in the acetonitrile complexes (Figure 2). A three-band pattern in the carbonyl stretching region of the

(15) Smith, M. B.; Bau, R. *J. Am. Chem. Soc.* **1973**, *95*, 2388.
(16) (a) Sosinsky, B. A.; Shong, R. G.; Fitzgerald, B. J.; Norem, N.; O'Rourke, C. *Inorg. Chem.* **1983**, *22*, 3124. (b) Alvarez, S.; Ferrer, M.; Reina, R.; Rossell, O.; Seco, M.; Solans, X. *J. Organomet. Chem.* **1989**, *377*, 291.
(17) (a) Chin, H. B.; Bau, R. *J. Am. Chem. Soc.* **1976**, *98*, 2434. (b) Teller, R. G.; Finke, R. G.; Collman, J. P.; Chin, H. B.; Bau, R. *J. Am. Chem. Soc.* **1977**, *99*, 1104.
(18) White, J. P., III; Deng, H.; Shore, S. G. *Inorg. Chem.* **1991**, *30*, 2337.
(19) White, J. P., III; Deng, H.; Shore, S. G. *J. Am. Chem. Soc.* **1989**, *111*, 8946.
(20) Tilley, T. D.; Andersen, R. A.; Spencer, B.; Zalkin, A. *Inorg. Chem.* **1982**, *21*, 2647.
(21) Wayda, A. L.; Mukerji, I.; Dye, J. L.; Rogers, R. D. *Organometallics* **1987**, *6*, 1328.
(22) Darensbourg, M. Y. *Prog. Inorg. Chem.* **1985**, *33*, 221.

IR spectrum of an $Fe(CO)_4$ unit is indicative of C_{3v} symmetry, while a single band is indicative of tetrahedral symmetry. Local C_{3v} geometry of $Fe(CO)_4$ would result from the occupation of an axial site by a Yb^{2+} ion in a trigonal-bipyramidal $YbFe(CO)_4$ coordination sphere, similar to that of the $Fe(CO)_4$ unit in $\{[(CH_3CN)_3YbFe(CO)_4]_2\cdot CH_3CN\}_\infty$ and $[(CH_3CN)_3YbFe(CO)_4]_\infty$.

The $[HFe(CO)_4]^-$ anion has C_{3v} symmetry.[15] Its IR spectrum contains three bands in the carbonyl stretching region (Nujol mull of $K[HFe(CO)_4]$: 2017 w, 1928 m, br, 1835 s, br cm^{-1}). They are *ca.* 100 cm^{-1} higher than those observed in the spectra of $(NH_3)_2YbFe(CO)_4$ and the acetonitrile complexes. It is unlikely that $[HFe(CO)_4]^-$ is responsible for the Nujol mull IR spectra produced by the ammonia and acetonitrile complexes of $YbFe(CO)_4$, since the MAS solid state ^2H NMR spectra of $(N^2H_3)_2YbFe(CO)_4$ ($\delta = 1.05$ ppm) do not give any indication for the presence of $[^2HFe(CO)_4]^-$ ($\delta = -11.2$ ppm) in the solid material. Only the ^2H in the coordinated, deuterated ammonia is observed. Therefore we believe that the solid state structure of $(NH_3)_2YbFe(CO)_4$ very likely mimics the structures of the acetonitrile derivatives.

Comparison of $\{[(CH_3CN)_3YbFe(CO)_4]_2\cdot CH_3CN\}_\infty$ and $[(CH_3CN)_3YbFe(CO)_4]_\infty$ in Solution and in the Solid State. Just as the MAS solid state NMR spectrum of $(N^2H_3)_2YbFe(CO)_4$ gives no evidence for the presence of $[^2HFe(CO)_4]^-$, the MAS solid state NMR spectra of the acetonitrile-d_3 complexes ($\delta = 1.05$ ppm) also give no indication of the presence of $[^2HFe(CO)_4]^-$ ($\delta = -11.2$ ppm). Only the deuterium in the coordinated acetonitrile is observed. However, when single crystals of the acetonitrile complexes are dissolved in acetonitrile, the presence of $[HFe(CO)_4]^-$ is detected in both infrared and NMR spectra. These observations imply that an equilibrium exists between ionic species in solution and polymeric covalent species in the solid state identified by the X-ray structural studies. Electrical conductance measurements of $\{[(CD_3CN)_3YbFe(CO)_4]\cdot CD_3CN\}_\infty$ in acetonitrile solution over the concentration range $8.8 \times 10^{-4}-9.6 \times 10^{-4}$ M gives Λ_m 86.2 Ω^{-1} cm^2 mol^{-1}, which falls below the range usually observed for 1:1 electrolytes in CH_3CN solution (Λ_m 120−160 Ω^{-1} cm^2 mol^{-1}).[23] Thus it appears that $\{[(CD_3CN)_3YbFe(CO)_4]\cdot CD_3CN\}_\infty$ is not completely dissociated in CH_3CN solution. In solution, rupture of the Yb−Fe bond could occur to generate the ion pair $[L_nYb]^{2+}[Fe(CO)_4]^{2-}$, but then the highly basic $[Fe(CO)_4]^{2-}$ anion could abstract a proton from a coordinated acetonitrile ligand to form $[HFe(CO)_4]^-$. However, upon crystallization, the proton could be transferred back to the ligand, which would result in the neutral polymeric species. We have not been able to identify CH_2CN^- either in solution or as a coordinated ligand. However, we have shown that $[Fe(CO)_4]^{2-}$ induces catalytic exchange of deuterium and protium in CD_3CN-CH_3CN mixtures. The exchange process undoubtedly occurs through the initial deprotonation of the acetonitrile to form the $[HFe(CO)_4]^-$ intermediate.[24]

Experimental Section

General Data. All manipulations were carried out on a standard high-vacuum line or in a drybox under an atmosphere of dry, pure N_2. CH_3CN was dried over P_4O_{10} with continuous stirring for 5 days, followed by distillation into storage bulbs. CD_3CN (99.96% atomic deuterium, Isotec Inc.) was used as received. NH_3 (Matheson) was dried over sodium and distilled prior to use. ND_3 was prepared from D_2O (Aldrich), and Mg_3N_2 (Alfa) and was dried over sodium.

Yb (40 mesh, Strem Chemicals) was used as received. $Fe_3(CO)_{12}$ (Strem Chemicals) was recrystallized from CH_2Cl_2, dried, and stored in the drybox.

$KHFe(CO)_4$ and $KDFe(CO)_4$ were prepared from $K_2Fe(CO)_4$ and HCl or DCl according to a modified literature method.[25]

All IR spectra were recorded with 2 cm^{-1} resolution using a Mattson-Polaris FT-IR spectrometer. Solution spectra were obtained in Perkin-Elmer liquid cells with 0.1 mm Teflon spacers and KBr windows. Proton NMR (δ(TMS) = 0.00 ppm) spectra were obtained at 300 K on either a Bruker AM-250 NMR spectrometer operating at 250.14 MHz or a Bruker AC-300 NMR spectrometer operating at 300.13 MHz. All chemical shifts are reported in δ (ppm). Elemental analyses were performed by Oneida Research Services, Whitesboro, NY. Solid state MAS ^2H NMR spectra were obtained on a Chemagnetics CMX400 NMR spectrometer operating at 9.4 T (^2H frequency of 61.4 MHz) using a home-built MAS probe with sample-spinning rates between 11 and 12 kHz. All spectra were acquired with a spectral width of 300 kHz and a pulse angle of approximately $\pi/3$ and were referenced to CD_3CN. Electrical conductance measurements were obtained using a Yellow Springs Instrument Co. (YSI) Model 35 conductance−resistance meter equipped with a YSI Model 3401 dip cell. All measurements were performed in the drybox employing standardized solutions in CH_3CN.

Preparation of $(NH_3)_2YbFe(CO)_4$. In the drybox a 50 mL flask was charged with 173 mg (1.00 mmol) of Yb, 168 mg (0.33 mmol) of $Fe_3(CO)_{12}$, and a magnetic stir bar. The flask was connected to a vacuum adapter, which was connected to the vacuum line and evacuated. Ammonia, 20 mL was condensed into the flask at −78 °C. The reaction mixture was allowed to warm slightly, and the blue color of solvated electrons was immediately noticed. The solution was stirred for 20 min with occasional cooling of the flask at −78 °C. During this time, the solution changed color from blue to green and then yellow, with the formation of a yellow solid. The ammonia was then removed under vacuum. The product was obtained in near-quantitative yield. The product was washed with CH_3CN in order to remove a very small amount of unidentified impurities (at the same time some product is lost due to slight solubility in CH_3CN). Thus 10 mL of CH_3CN was distilled into the flask at −78 °C. The flask was brought into the drybox and was attached to an vacuum extractor. The suspension of the yellow solid in CH_3CN was filtered, and then CH_3CN was removed under vacuum. The yellow solid collected on the frit was dried under vacuum for 2 h. It is extremely air- and moisture sensitive, as the surface of the solid changes color to brown over a couple of weeks in a well-maintained drybox. Yield: 280 mg, 75%. IR (Nujol mull, cm^{-1}): 3345 (w), 3265 (w) (ν_{NH}); 1898 (w), 1826 (m), 1758 (s) (ν_{CO}). Anal. Calcd for $C_4H_{5.4}FeN_{1.8}O_4Yb$: C, 12.93; H, 1.46; N, 6.79. Found: C, 12.99; H, 1.42; N, 6.94. $(ND_3)_2YbFe(CO)_4$ was prepared similarly in liquid ND_3. IR (Nujol mull, cm^{-1}): 2496 (w) (ν_{ND}); 1898 (w), 1812 (m, sh), 1746 (s) (ν_{CO}). ^2H MAS NMR: δ 1.05 ppm.

NMR Spectra in Acetonitrile. $(NH_3)_2YbFe(CO)_4$ in CD_3CN (99.96% atomic deuterium) ^1H NMR: δ 1.96 (q, $J_{H-D} = 2.5$ Hz, residual CHD_2CN), −8.96 (s, $[HFe(CO)_4]^-$).

Preparation of $\{[(CH_3CN)_3YbFe(CO)_4]_2\cdot CH_3CN\}_\infty$. A 10 mL portion of CH_3CN was added to a freshly prepared sample of $(NH_3)_2YbFe(CO)_4$. The mixture was stirred for 10 min and filtered. The volume of the orange filtrate was reduced until small crystals could be seen. The filtrate was then placed in a −40 °C refrigerator for about 2 weeks. About a dozen orange needle-like crystals were obtained. IR (Nujol mull, ν_{CO}, cm^{-1}): 1890 (m), 1781 (m, sh), 1720 (s). Anal. Calcd for $C_{22}H_{21}Fe_2N_7O_8Yb_2$: C, 27.19; H, 2.18; N, 10.10. Found: C, 26.80; H, 2.08; N, 10.22. $\{[(CD_3CN)_3YbFe(CO)_4]_2\cdot CD_3CN\}_\infty$ was prepared similarly in CD_3CN from fresh $(ND_3)_2YbFe(CO)_4$. ^2H MAS NMR: δ 0.65 ppm.

Preparation of $[(CH_3CN)_3YbFe(CO)_4]_\infty$. A freshly prepared sample of $(NH_3)_2YbFe(CO)_4$ in a minimal amount of liquid NH_3 was quenched by 15 mL of CH_3CN (distilled into the flask at −78 °C), and the mixture was stirred for 10 min at room temperature. All volatiles were then removed under vacuum. A 10 mL portion of fresh CH_3CN was distilled into the flask, and the mixture was filtered. The volume of the orange filtrate was reduced until small crystals could be seen. The filtrate was then placed in a −40 °C refrigerator for about

(23) Geary, W. J. *Coord. Chem. Rev.* **1971**, *7*, 81.
(24) Deng, H. Unpublished observation.
(25) (a) Darensbourg, M. Y.; Darensbourg, D. J.; Barros, H. L. C. *Inorg. Chem.* **1978**, *17*, 297. (b) Walker, H. W.; Ford, P. C. *J. Organomet. Chem.* **1981**, *214*, C43.

2 weeks, and about a dozen orange single crystals of $[(CH_3CN)_3YbFe(CO)_4]_\infty$ were obtained. IR (Nujol mull, ν_{CO}, cm^{-1}): 1890 (m), 1794 (m), 1715 (s). Anal. Calcd for $C_{10}H_9FeN_3O_4Yb$: C, 25.81; H, 1.95; N, 9.04. Found: C, 24.97; H, 2.08; N, 8.88.

X-ray Structure Determination of $\{[(CH_3CN)_3YbFe(CO)_4]_2\cdot CH_3CN\}_\infty$. The structure of $\{[(CH_3CN)_3YbFe(CO)_4]_2\cdot CH_3CN\}_\infty$ was reported in our preliminary study.[7] Crystal data and important bond distances and angles are listed in Tables 1 and 2, respectively.

X-ray Structure Determination of $[(CH_3CN)_3YbFe(CO)_4]_\infty$. Crystals of suitable size were coated with epoxy resin in the drybox and glued to the tips of glass fiber. All crystallographic data were collected on an Enraf-Nonius CAD4 diffractometer with graphite-monochromated Mo Kα radiation. Unit cell parameters were obtained by a least-squares refinement of the angular settings of 25 reflections, well distributed in reciprocal space and lying in a 2θ range of 24−30°. The diffraction symmetry (C_{2h}, 2/*m*) and the systematic absences (*h*0*l* for $h + l = 2n+1$; 0*k*0 for $k = 2n+1$) uniquely determine the space group $P2_1/n$ (No. 14). Crystallographic data are given in Table 1, and bond distances and angles are given in Table 2. Positional and equivalent isotropic thermal parameters are given in Table 3.

The diffraction data were corrected for Lorentz and polarization effects, decay, and absorption (empirically from ψ-scan data). The structure was solved by employing a combination of MULTAN 11/82 and difference Fourier techniques with analytical scattering factors used throughout the structure refinement and both real and imaginary components of the anomalous dispersion included for all non-hydrogen atoms. All crystallographic computations were carried out on a DEC Vax station 3100 computer, using the Structure Determination Package (SDP).[26] After all of the non-hydrogen atoms were located and refined, one hydrogen atom for every acetonitrile methyl group was located from difference Fourier maps and the remaining hydrogen atoms on the CH_3CN ligands were placed at calculated positions by assuming ideal geometries with d(C−H) = 0.95 Å and B(H) = 1.3B(C) Å^2. Then with the positional and thermal parameters of all of the hydrogens fixed, the non-hydrogen atoms were refined anisotropically (atoms O1, C3, and C4 were refined isotropically as they became non-positive definite after anisotropic refinement; crystal decomposition during data collection (intensity loss is 33%) is probably responsible for this). New hydrogen positions were calculated, and this procedure was repeated until the parameters of non-hydrogen atoms were refined to convergence (final shift/error ≤ 0.03). The highest residual peak on the final difference Fourier map is 1.52 e/Å^3 except those within 1.3 Å of Yb and Fe atoms (with maximum density of 5.21 e/Å^3).

(26) SDP (developed by B. A. Frenz and Associates, Inc., College Station, TX 77840) was used to process X-ray data, to apply corrections, and the solve and refine structures.

(27) The average distance is the mean of several values, and the esd shown in brackets is calculated from $[\sum_{i=1}^{N}(d_i - \bar{d})^2/(N-1)]$, where d_i is the ith value and $\bar{d}$ is the mean of N values.

Table 3. Positional and Equivalent Isotropic Thermal Parameters and Their Estimated Standard Deviations for $[(CH_3CN)_3YbFe(CO)_4]_\infty$[a]

atom	*x*	*y*	*z*	*B*, Å^2
Yb	0.64132(7)	0.23814(5)	0.80763(3)	1.36(1)
Fe	0.0045(2)	0.2440(2)	0.7999(1)	1.22(3)
O1	0.350(1)	0.2432(9)	0.8153(6)	2.8(2)[b]
O2	−0.084(1)	0.478(1)	0.6987(6)	3.1(2)
O3	−0.071(2)	−0.046(1)	0.7622(7)	3.4(3)
O4	−0.032(2)	0.300(2)	0.9645(7)	5.0(3)
N1	0.625(2)	0.442(1)	0.9022(7)	3.0(3)
N2	0.642(2)	0.127(1)	0.9431(8)	3.1(3)
N3	0.546(2)	0.173(1)	0.6694(8)	3.3(3)
C1	0.211(2)	0.242(1)	0.8041(8)	1.5(2)
C2	−0.057(2)	0.380(1)	0.7403(9)	2.5(3)
C3	−0.046(2)	0.074(1)	0.7753(9)	2.4(3)[b]
C4	−0.025(2)	0.276(1)	0.8980(9)	2.8(3)[b]
C11	0.639(2)	0.551(2)	0.9234(9)	2.7(3)
C12	0.659(2)	0.695(2)	0.951(1)	3.8(4)
C21	0.694(2)	0.087(2)	1.0002(9)	2.9(4)
C22	0.759(3)	0.037(2)	1.076(1)	5.5(5)
C31	0.428(2)	0.131(2)	0.6405(9)	2.9(3)
C32	0.276(2)	0.081(2)	0.610(1)	3.9(4)
H1	0.7929	0.7207	0.9570	5[c]
H2	0.8339	−0.0566	1.0742	7[c]
H3	0.2500	−0.0293	0.6035	5[c]
H4	0.6123	0.7040	1.0005	4[c]
H5	0.6072	0.7569	0.9155	4[c]
H6	0.6707	0.0167	1.1072	7[c]
H7	0.8207	0.1096	1.0987	7[c]
H8	0.2622	0.1199	0.5591	5[c]
H9	0.1972	0.1176	0.6422	5[c]

[a] Anisotropically refined atoms are given in the form of the isotropic equivalent displacement parameter defined as $(4/3)[a^2\beta(1,1) + b^2\beta(2,2) c^2\beta(3,3) + ab(\cos\gamma)\beta(1,2) + ac(\cos\beta)\beta(1,3) + bc(\cos\alpha)\beta(2,3)]$. [b] Refined isotropically. [c] Hydrogen atoms H1, H2, and H3 were located from difference Fourier maps, and the remaining ones were calculated at d(C−H) = 0.95 Å; their thermal parameters were assigned to B(H) = 1.3B(C) Å^2.

Acknowledgment. This work was supported by the National Science Foundation through Grant CHE 94-0123.

Supporting Information Available: Listings of additional X-ray experimental details and anisotropic thermal parameters for $[(CH_3CN)_3YbFe(CO)_4]_\infty$ (2 pages). Ordering information is given on any current masthead page. Analogous Supporting Information for $\{[(CH_3CN)_3YbFe(CO)_4]_2\cdot CH_3CN\}_\infty$ is given elsewhere.[7]

IC9515113